Detection of Nucleotide- and F-Actin-Induced Movements in the Switch II Helix of the Skeletal Myosin Using Its Differential Oxidative Cleavage Mediated by an Iron−EDTA Complex Disulfide-Linked to the Strong Actin Binding Site†

Raoul Bertrand, Jean-Paul Capony, Jean Derancourt, and Ridha Kassab*

Centre de Recherches de Biochimie Macromoléculaire du CNRS, UPR 1086, 1919 Route de Mende, 34293 Montpellier Cedex 5, France

Received April 30, 1999; Revised Manuscript Received July 7, 1999

ABSTRACT: We have synthesized the mixed disulfide, *S*-(2-nitro-5-thiobenzoic acid) cysteaminyl-EDTA, using a rapid procedure and water-soluble chemistry. Its disulfide−thiol exchange reaction with rabbit myosin subfragment-1 (S-1), analyzed by spectrophotometry, ATPase assays, and peptide mapping, led to the incorporation of the cysteaminyl-EDTA group into only Cys 540 on the heavy chain and into the unique cysteine on the alkali light chains. The former thiol, residing in the strong actin binding site, reacted at a much faster rate with a concomitant 3-fold decrease in the V_{max} for acto-S-1 ATPase but without change in the essential enzymatic functions of S-1. Upon chelation of Fe^{3+} ions to the Cys 540-bound EDTA and incubation of the S-1 derivative−Fe complex with ascorbic acid at pH 7.5, the 95 kDa heavy chain underwent a conformation-dependent, single-cut oxidative fragmentation within 5−15 Å of Cys 540. Three pairs of fragments were formed which, after specific fluorescent labeling and SDS−PAGE, could be positioned along the heavy chain sequence as 68 kDa−26 kDa, 62 kDa−32 kDa, and 54 kDa−40 kDa. Densitometric measurements revealed that the yield of the 54 kDa−40 kDa pair of bands, but not that for the two other pairs, was very sensitive to S-1 binding to nucleotides or phosphate analogues as well as to F-actin. In binary complexes, all the former ligands specifically lowered the yield to 40% of S-1 alone, roughly in the following order: ADP = AMP-PNP > ATP = ADP·AlF_4 > ADP·BeF_x > PP_i. By contrast, rigor binding to F-actin increased the yield to 130%. In the ternary acto-S-1−ADP complex, the yield was again reduced to 80%, and it fell to 25% in acto-S-1−ADP·AlF_4, the putative transition state analogue complex of the acto-S-1 ATPase. These different quantitative changes reflect distinct ligand-induced conformations of the secondary structure element whose scission generates the 54 kDa−40 kDa species. According to the S-1 crystal structure, this element could be unambiguously assigned to the switch II helix (residues 475−507) whose N-terminus lies 14.2 Å from Cys 540 and would include the ligand-responsive cleavage site. This motif is thought to be crucial for the transmission of sub-nanometer structural changes at the ATPase site to both the actin site and the lever arm domain during energy transduction. Our study illustrates this novel, actin site-specific chemical proteolysis of S-1 as a direct probe of the switch II helix conformational transitions in solution most likely associated with the skeletal cross-bridge cycle.

Force production in muscle and many other motile systems is accomplished by the cyclical interactions between the globular heads of myosin (S-1)[1] and F-actin which are coupled with ATP hydrolysis. The crystal structure of skeletal S-1 shows that this motor protein consists of a catalytic domain, containing the actin- and nucleotide-binding sites, attached to an 8 nm long α-helical C-terminal domain associated with light chains (*1*). The structural models of the acto-S-1 complex, based on S-1 X-ray structures with various bound nucleotides and transition state analogues, have suggested a molecular mechanism of energy transduction via this complex, implying that small conformational changes in the nucleotide-hydrolyzing pocket are transmitted to and then magnified in the latter light chain binding helix which would act as a lever arm (*2*−*7*). Its wagging motion would cause the translocalization of S-1 along F-actin. This proposal and other three-dimensional reconstruction studies with the actomyosin complex (*8*) have placed critical importance on movements of secondary structure elements residing in the catalytic domain but converging at the base

† This research was supported by grants from the Centre National de la Recherche Scientifique and the Association Française contre les Myopathies.

* To whom correspondence and reprint requests should be addressed. Fax: 33 467 52 1559. E-mail: kassab@crbm.cnrs-mop.fr. Telephone: 33 467 61 3335.

[1] Abbreviations: S-1, myosin subfragment 1; acto-S-1, actomyosin subfragment 1; ATPase, adenosine 5′-triphosphatase; $NaDodSO_4$, sodium dodecyl sulfate; DTNB, 5,5′-dithiobis(2-nitrobenzoic acid); EDTA, ethylenediaminetetraacetic acid; NTB-cysteaminyl-EDTA, *S*-(2-nitro-5-thiobenzoic acid)cysteaminyl-EDTA; [(cysteaminyl-EDTA)-Cys]S-1, myosin subfragment 1 modified at cysteine with NTB-cysteaminyl-EDTA; 1,5-IAEDANS, *N*-(iodoacetyl)-*N*′-(5-sulfo-1-naphthyl)ethylenediamine; 5-IAF, 5-iodoacetamidofluorescein; NEM, *N*-ethylmaleimide; DTE, dithioerythritol; MOPS, 3-(*N*-morpholino)-propanesulfonic acid.

10.1021/bi9909896 CCC: $18.00
Published on Web 08/24/1999

of the lever arm region. These include, in particular, the helix containing the two reactive SH1−SH2 thiols and the highly conserved helix of residues 475−507, denoted the switch II helix. Both motifs, which were observed to move in crystal structures of truncated *Dictyostelium* S-1 bound to ADP·AlF_4 or ADP·Vi (*2*, *7*), are thought to represent potential communication routes conducting the modest nucleotide-induced conformational changes to the putative amplifier lever arm. Earlier, extensive biochemical solution studies have been used first to detect the structural changes of the SH1−SH2 helix of skeletal S-1 and to analyze their relationships with the various S-1−nucleotide intermediate states of the ATPase reaction, using, principally, chemical cross-linking approaches (*9*−*14*). Recent such investigations have revealed different conformational states of this helix which could not be observed in the three-dimensional atomic structures of S-1 (*15*). By contrast, to date, no investigations in solution were reported for the visualization of the conformation shifts specifically associated with the switch II helix of skeletal S-1 upon binding of nucleotides and or F-actin. This helix is of particular interest, as it exhibits the additional important property of running along the nucleotide- and F-actin-sensitive narrow cleft separating the lower and upper 50 kDa subdomains and to be positioned in spatial proximity of the U-shaped helix−loop−helix motif of residues 516−558 representing the primary stereospecific and hydrophobic strong actin binding surface of S-1 (*1*, *16*). This strategic location is thought to provide the switch II helix with the potential ability to also serve as a communication pathway between the actin- and nucleotide-binding sites. Thus, assessing its structural transitions in solution may help provide insight into the concerted nucleotide- and F-actin-dependent movements of the long lever arm helix.

Herein, we report, for the first time, an exprimental approach for directly probing in solution nucleotide- and/or F-actin-induced specific states of the switch II helix in rabbit skeletal S-1, using the conformation-dependent change in the amplitude of its oxidative cleavage catalyzed by a cysteaminyl-EDTA−Fe chelate which we have linked by a disulfide bond to Cys 540. This amino acid lies at the end of the first helix of the strong actin-binding motif and is located only about 14 Å from the N-terminus of the switch II helix (Leu 475). The cysteaminyl-EDTA group was delivered to Cys 540 of S-1 through the unprecedented selective thiol−disulfide interchange reaction, which we have characterized in this study, between this residue and a novel thiol-specific mixed disulfide, *S*-(2-nitro-5-thiobenzoic acid) cysteaminyl-EDTA, which we have synthesized in aqueous medium by a very fast and straightforward procedure. Earlier, the cysteaminyl-EDTA−Fe complex, convalently bound at a selected protein site, was demonstrated to promote, in the presence of ascorbic acid, the generation of reactive oxygen species around the iron atom that cause a site-specific limited proteolysis at solvent-exposed peptide bonds residing in the tertiary fold of the protein within a radius of 5−15 Å from the attachment site (*17*−*22*). This distance corresponds to the dynamic span of the cysteaminyl-EDTA−Fe group between the Cα of the latter site and the metal ion (*18*, *19*). Because the extent and/or location of this chemical cleavage is highly sensitive to protein conformation, it has been proposed as a powerful tool for monitoring, by the comparison of the protein fragmentation patterns, different conformational states of secondary structure elements which are in a three-dimensional structural proximity to the site of binding of the EDTA−Fe chelate (*18*). Our study describes the specific cleavage of the S-1 heavy chain at three secondary structure segments adjacent to Cys 540 substituted with the cysteaminyl-EDTA−Fe moiety and the specific modulation by nucleotides, phosphate analogues, and/or F-actin of the cleavage magnitude for only one of them. The molecular masses and positions along the heavy chain sequence for the pair of fragments generated by the ligand-responsive cleavage, combined with the knowledge of the S-1 crystal structure, strongly suggest that this proteolytic event took place at the N-terminal part of the switch II helix. Our data serve to reveal not only several distinct conformational states in solution of this functionally important motif but also the specific covalent labeling of the strong actin-binding site of skeletal S-1 with metal−EDTA chelates potentially useful for luminescence or fluorescence spectroscopy.

MATERIALS AND METHODS

Chemicals. Cysteamine hydrochloride and 5,5′-dithiobis-(2-nitrobenzoic acid) (DTNB) were obtained from Fluka. EDTA dianhydride and iron(III) chloride hexahydrate were supplied by Aldrich. Chymotrypsin and TPCK-treated trypsin were purchased from Worthington. *N*-(Iodoacetyl)-*N*′-(5-sulfo-1-naphthyl)ethylenediamine (1,5-IAEDANS) and *N*-ethylmaleimide (NEM) were purchased from Sigma. 5-Iodoacetamidofluorescein (5-IAF) was from Molecular Probes (Eugene, OR).

Proteins. Rabbit skeletal myosin was prepared as described previously (*23*). Chymotryptic S-1 (A1 and A2) was obtained according to ref *24*. F-Actin from rabbit skeletal muscle was prepared by the procedure described in ref *25*. S-1 was modified at Cys 707 with 1,5-IAEDANS or 5-IAF as described previously (*26*). Intramolecular cross-linking between Cys 522 and Cys 707 of S-1 was performed as reported earlier (*27*). Protein concentrations were determined spectrophotometrically at 280 nm with an extinction coefficient $A_{1\%}$ of 7.5 cm^{-1} for S-1 and 11.0 cm^{-1} for actin. The concentration of modified S-1 derivatives was calculated after subtracting the absorbance of the modifying group at this wavelength. The concentration of free nitrothiobenzoate ion was estimated at 412 nm using a molar extinction coefficient of 14 150 M^{-1} cm^{-1} (*28*).

Synthesis of S-(2-Nitro-5-thiobenzoic acid)cysteaminyl-EDTA (NTB-Cysteaminyl-EDTA). Cysteamine hydrochloride at a final concentration of 10.75 mM in 500 mM MOPS (pH 8.5) was reacted with a 1.1-fold molar excess of DTNB dissolved in dimethylformamide (620 mM). The mixture was stirred for 30 min at 20 °C. A spectrophotometric analysis at 412 nm indicated an almost 100% yield of NTB-cysteamine. EDTA dianhydride (150 mM) dissolved in dimethylformamide by heating at 95 °C was then added, under vigorous stirring, to a final concentration of 22.5 mM, using five equal aliquots each introduced after an interval of 15 min. The NTB-cysteaminyl-EDTA adduct that formed was isolated by reverse-phase HPLC. About 75 μL of this solution was mixed with 1 mL of 0.25% aqueous trifluoroacetic acid and loaded on an Aquapore C-8 Brownlee RP-300 column (4 mm × 220 mm) eluted for 60 min with a 0

to 75% acetonitrile gradient (solvent B) containing 0.1% trifluoroacetic acid (solvent A), at a flow rate of 1 mL/min and collecting 1 mL fractions. The absorbance of the effluent was monitored at 330 nm. The final mixed disulfide was eluted as a single peak at 25% acetonitrile just following the elution at 23% acetonitrile of the liberated nitrothiobenzoate ion. Its precursor, NTB-cysteamine, was completly absent in this chromatographic profile, but when the addition of EDTA dianhydride was omitted, it was eluted as a single peak at 18% acetonitrile. The chemical structure of NTB-cysteamine-EDTA was confirmed by ionization mass spectrometry which showed a unique product with a molecular mass of 548.9 Da (calculated mass of 548.54 Da). Its concentration was measured spectrophotometrically at 412 nm after incubation in 50 mM NaOH for 1 h at 20 °C. This assay revealed that at least 75% of the starting cysteamine was recovered as NTB-cysteaminyl-EDTA. After several similar chromatographic runs, the accumulated material was fractionated into 1 mL aliquots which were dried with a Speed Vac centrifuge and stored at −20 °C.

Derivatization of S-1 and Cleavage Reactions. S-1 (3−50 μM) in 20 mM MOPS (pH 8.0) was mixed with a 1.1−4.35-fold molar excess of NTB-cysteaminyl-EDTA dissolved immediately before use in 50 mM Tris-HCl (pH 7.2) at a concentration of 500 μM. The reaction was monitored at 412 nm for 3 h at 20 °C. In parallel, protein aliquots were withdrawn at various time intervals and subjected to ATPase measurements or to the oxidative cleavage reaction. To initiate the latter process, the sample was first incubated for 30 min at 20 °C with aqueous $FeCl_3 \cdot 6H_2O$ (20 mM) added at a 2-fold molar excess over NTB-cysteaminyl-EDTA. The fragmentation of the resulting [(cysteaminyl-EDTA−Fe)-Cys]S-1 was then carried out by adding an aqueous solution of ascorbic acid (200 mM), adjusted to pH 7.2 with Tris, to give a final concentration of 15 mM. It was conducted in the absence and in the presence of ATP, ADP, AMP, AMP-PNP, PP_i, ADP·AlF_4, ADP·BeF_x, or F-actin; the latter protein was employed alone or in combination with ADP or ADP·AlF_4. Cleavage was also carried out in the presence of 0.5% $NaDodSO_4$. After 30−60 min at 20 °C, the reaction was terminated by adding β-mercaptoethanol to a final concentration of 4% (v/v). The cleavage patterns were established by $NaDodSO_4$−acrylamide gel electrophoresis.

Identification of the S-1 Cysteines Modified with NTB-Cysteaminyl-EDTA. S-1 (50 μM) in 20 mM MOPS (pH 8.0) was treated for 3 h at 20 °C with a 2.5-fold molar excess of NTB-cysteaminyl-EDTA. The pH of the solution was brought to 7.0 by adding MOPS (500 mM, pH 7.0) to a final concentration of 50 mM. The mixture was then treated with NEM according to the method of Gitler et al. (*29*) to achieve the specific fluorescent labeling of S-1 thiol(s) converted to a disulfide state upon substitution with the cysteaminyl-EDTA group. NEM dissolved in dimethylformamide (250 mM) was added at a 5-fold molar excess over total S-1 thiols. After 15 min at 20 °C, the temperature of the solution was lowered to 0 °C in an ice bath and $NaDodSO_4$ was added to a final concentration of 0.5%. After 30 min at 0 °C, the modified S-1 was gel filtered over a NAP-10 column (Pharmacia) eluted at 20 °C with 40 mM MOPS, 0.05% $NaDodSO_4$, and 0.1 mM EDTA (pH 8.5). The protein fraction was submitted to reduction for 60 min at 37 °C with 5 mM DTE and then refiltered over the same column eluted with 20 mM MOPS, 0.01% $NaDodSO_4$, 0.1 mM DTE, and 0.1 mM EDTA (pH 8.0). To the collected S-1 solution was added 5-IAF, dissolved in dimethylformamide (100 mM), to a final concentration of 4 mM. After 75 mn at 20 °C, the alkylation reaction was quenched by adding DTE to a final concentration of 7.5 mM. After 10 min at 20 °C, the mixture was passed over a NAP-10 column eluted with 20 mM MOPS and 0.01% $NaDodSO_4$ (pH 8.0).

One milliliter of the IAF−S-1 preparation (16 μM) was first subjected to reverse-phase HPLC on an Aquapore C-8 Brownlee column (4 mm × 220 mm) for the isolation of pure fluorescent S-1 heavy chain and alkali light chains. Linear gradient elution was performed for 60 min with 0 to 100% solvent B consisting of 75% acetonitrile in 0.1% aqueous trifluoroacetic acid (solvent A). The flow rate was adjusted to 1 mL/min, and 1 mL fractions were collected. The pH of an aliquot (100 μL) of each fraction was brought to 8.5 by the addition of 1 μL of 5 M NaOH, and the fluorescence was monitored at 520 nm with excitation at 495 nm. The separated heavy chain and light chain fractions were then pooled, dried with a Speed Vac centrifuge, resuspended in 500 μL of 250 mM Tris-HCl and 2 M urea (pH 8.0), and digested at 37 °C for 2 h with chymotrypsin and trypsin, respectively, at an enzyme:substrate weight ratio of 1:20. Each digest was finally fractionated on an Aquapore C-8 Brownee column (4 mm × 220 mm) using the same experimental conditions described above. The fluorescent peptides were further purified on a Brownlee C-18 column (2 mm × 100 mm) eluted for 60 min with 0 to 100% solvent B consisting of 60% acetonitrile in 0.1% trifluoroacetic acid (solvent A) at a flow rate of 200 μL/min and collecting 0.2 mL fractions.

Amino acid sequencing of the pure fluorescent peptides was conducted using a Perkin-Elmer Procise 492 Sequencer operating according to the manufacturer's pulsed liquid program. Their molecular mass values were determined by electrospray ionization mass spectrometry on a VG Trio-2000 mass spectrometer as previously described (*30*).

ATPase Assays. The Ca^{2+}−ATPase activities were measured at 25 °C in the presence of 2.5 mM ATP, 250 mM KCl, 5 mM $CaCl_2$, and 50 mM Tris-HCl (pH 7.7). The K^+−EDTA ATPase activities were determined at 25 °C in 2.5 mM ATP, 1 M KCl, 5 mM EDTA, and 50 mM Tris-HCl (pH 7.5). The Mg^{2+}−ATPase and actin-activated ATPase activities were assayed by incubating the S-1 in 5 mM ATP, 2.5 mM $MgCl_2$, 10 mM KCl, and 50 mM Tris-HCl (pH 8.0) in the absence and presence of varying concentrations (0.5−1.0 mg/mL) of F-actin, respectively. Inorganic phosphate was estimated colorimetrically according to the method described in ref *31*.

Electrophoresis. $NaDodSO_4$−polyacrylamide gradient gel electrophoresis (5 to 18%) was carried out as previously described (*31*, *32*). Fluorescent bands were located in the gels by illumination with a long-wavelength ultraviolet light before staining with Coomassie blue. Densitometric scanning of the gels was performed with a Schimadzu model CS-930 high-resolution gel scanner equipped with a computerized integrator. The following proteins, including various S-1 polypeptides to maximize the correlation between size and mobility, were used as molecular mass markers: S-1 heavy chain (95 000 Da), serum albumin (68 000 Da), the central tryptic fragment of the S-1 heavy chain (48 000 Da), actin

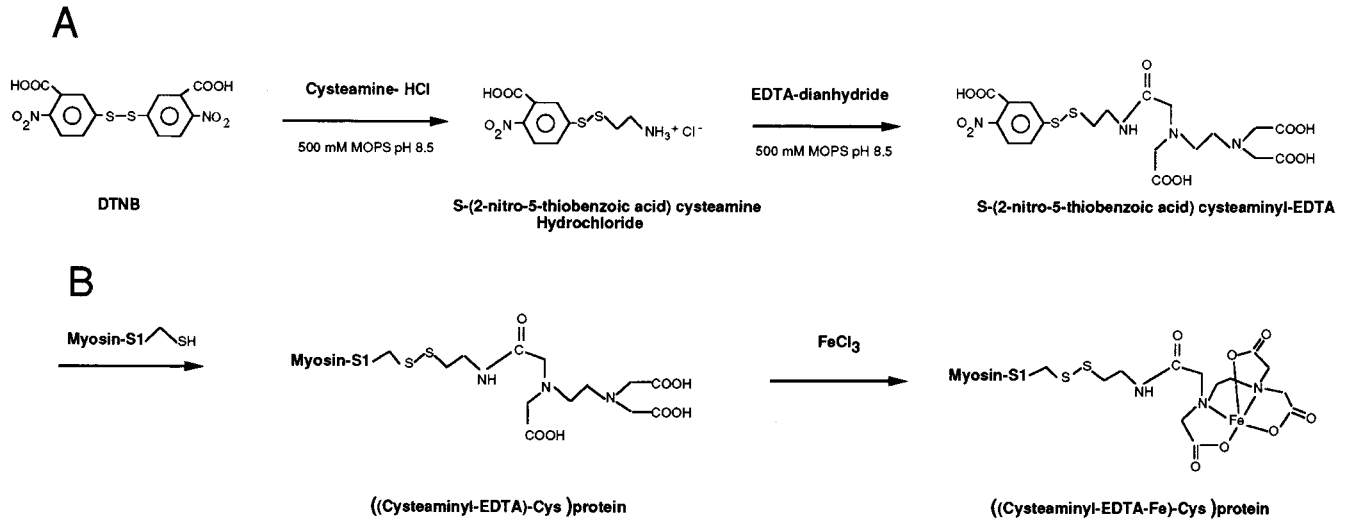

FIGURE 1: Schematic representation of the two-step synthesis of *S*-(2-nitro-5-thiobenzoic acid)cysteaminyl-EDTA (A) and the subsequent production of [(cysteaminyl-EDTA−Fe)Cys]S-1 (B).

(42 000 Da), chymotrypsinogen A (25 000 Da), soybean trypsin inhibitor (21 000 Da), the C-terminal tryptic fragment of the S-1 heavy chain (20 000 Da), and alkali light chain 2 (16 500 Da).

RESULTS

Disulfide Exchange Reaction between Myosin S-1 and S-(2-Nitrobenzoic acid)cysteaminyl-EDTA. Using the simple two-step procedure depicted schematically in Figure 1A, the DTNB reagent could be easily and with high yield converted in aqueous solution, at pH 8.5, into *S*-(2-nitrobenzoic acid)-cysteaminyl-EDTA. Milligram amounts of this mixed disulfide could be isolated within 1 working day for derivatization of S-1 into [(cysteaminyl-EDTA)Cys]protein by a disulfide−thiol interchange reaction (Figure 1B). The additional chelation of Fe^{3+} ions to the latter derivative for subsequent oxidative proteolysis was achieved following the characterization of the disulfide exchange process with respect to its kinetics, stoichiometry, and effects on the S-1 enzymatic functions and the identification of the modified cysteine(s) in the S-1 primary structure.

Figure 2 shows the reaction time course at pH 8.0 and room temperature of S-1 with varying concentrations of *S*-(2-nitrobenzoic acid)cysteaminyl-EDTA, using a 1.1−4.35-fold molar excess of reagent over the protein. The disulfide exchange was monitored spectrophotometrically at 412 nm by evaluating the amount of 2-nitro-5-thiobenzoate anion that was released. As reported earlier, the mixed disulfides resulting from the reaction between DTNB and low-molecular mass thiol compounds, such as cysteamine, often generate, upon reaction with protein sulfhydriles, the same amount of nitrothiobenzoate anion as the parent DTNB (*33*). Thus, the absorbance we measured at 412 nm is likely to be closely related to the number of cysteaminyl-EDTA groups incorporated into S-1. Under the experimental conditions that were employed, maximally 2 thiols/mol of S-1 could be titrated after incubation for 300 min. However, all titration curves were clearly biphasic, suggesting that the two thiols have distinct chemical reactivities toward the mixed disulfide. One thiol exhibited an enhanced reaction rate, and its substitution was almost completed in less than 60 min at a

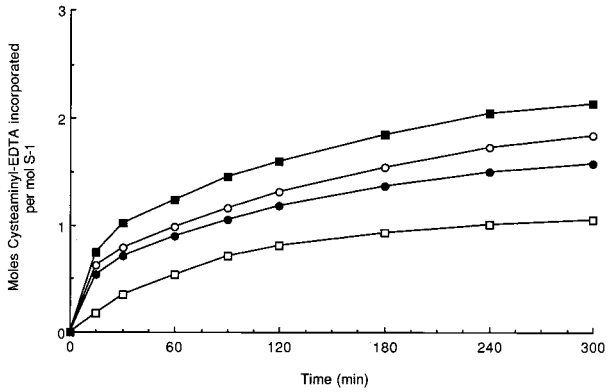

FIGURE 2: Time course of the covalent incorporation of the cysteaminyl-EDTA group into myosin S-1. The protein (3 μM) in 20 mM MOPS (pH 8.0) was reacted at 20 °C with a 1.1-fold (□), 2.15-fold (●), 3.25-fold (○), or 4.35-fold (■) molar excess of NTB-cysteaminyl-EDTA. The disulfide−thiol exchange was monitored by spectrophotometric measurements at 412 nm, and the extent of S-1 modification was estimated from the amount of nitrothiobenzoate ion released.

2−4-fold molar excess of reagent over S-1. By contrast, the reaction of the second thiol was much slower at all the reagent concentrations that were used, and it required an at least 4-fold molar excess of reagent over S-1 to go to completion.

Selective Inhibition of the Acto-S-1 ATPase by S-(2-Nitrobenzoic acid)cysteaminyl-EDTA. We then investigated the influence of the S-1 derivatization with the cysteaminyl-EDTA upon all its enzymatic activities during the entire course of the disulfide exchange reaction, using a constant reagent to S-1 molar ratio of 1.25. The results, presented in Figure 3, show that the K^+−, Ca^{2+}−, or Mg^{2+}−ATPase activities remained unchanged after reaction for 120 min with the rapid incorporation of about 1.0 mol of cysteaminyl-EDTA/mol of S-1. By contrast, during the same period, the acto-S-1 ATPase did undergo a progressive decrease to 25% of the control at the same rate as the chemical reaction. This 75% extent of inhibition plateaued for the remaining incubation time up to 300 min with a final modification of about 1.15 thiols/mol of S-1. Figure 4 illustrates the relationship found between the observed level of acto-S-1 ATPase

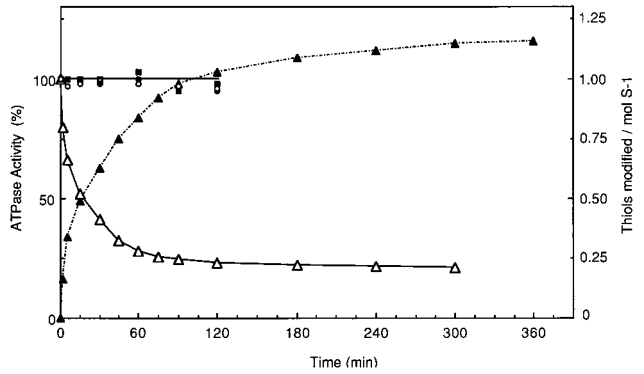

FIGURE 3: Influence of S-1 substitution with cysteaminyl-EDTA on its enzymatic activities. S-1 (45 μM) was incubated with a 1.25-fold molar excess of NTB-cysteaminyl-EDTA in 20 mM MOPS (pH 8.0) at 20 °C. At the indicated time intervals, protein samples were withdrawn and assayed for K^+−ATPase (●), Ca^{2+}−ATPase (○), Mg^{2+}−ATPase (■), and actin-activated ATPase (△). The enzymatic activities were measured as described in Materials and Methods. In parallel, the number of derivatized S-1 thiols (▲) was spectrophotometrically determined as described in the legend of Figure 2.

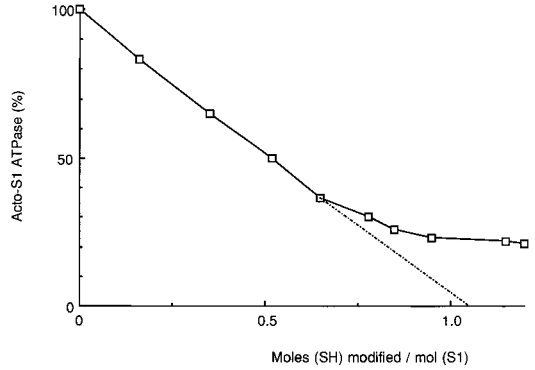

FIGURE 4: Relationship between the stoichiometry of thiol group modification in S-1 and the degree of acto-S-1 ATPase inhibition. Treatment of S-1 with NTB-cysteaminyl-EDTA with concomitant measurements of the acto-S-1 ATPase activities and titration of the number of modified SH groups per mole of S-1 were conducted as described in the legend of Figure 3.

reduction and the estimated number of S-1 thiols which have incorporated the cysteaminyl-EDTA group during the overall course of the reaction. Up to 0.70 thiol substituted/mol of S-1, there was a very close correlation between the degree of acto-S-1 ATPase inhibition and the fraction of reacting thiol with 100% inactivation extrapolated at nearly 1.0 thiol modified/mol of S-1. The findings clearly indicate that S-1 treatment with a molar excess of the reagent slightly larger than 1 results in the extensive inhibitory modification of a primary fast reacting thiol together with the marginal noninhibitory substitution of a second slowly reacting sulfhydrile. This conclusion is consistent with the initially observed kinetics of the disulfide exchange reaction. Double-reciprocal plots of the actin-activated ATPases of native S-1 and S-1 with 1.15 mol of attached cysteaminyl-EDTA, presented in Figure 5, indicated no change in the K_m for actin (130 μM), whereas the V_{max} value for the modified S-1 was decreased 2.5-fold (5.0 vs 12.2 s^{-1}). The overall data have several important implications. (1) The reaction of S-1 with NTB-cysteaminyl-EDTA did not alter ATP binding or hydrolysis at the ATPase site. This feature has a significant impact, with regard to the study reported below, on the influence of nucleotides on the oxidative fragmentation of the S-1 heavy chain. (2) In strong contrast to the parent DTNB (*12*), the mixed disulfide did not react at all with the reactive SH1 or SH2 thiols of S-1, but rather, it did specifically modify a different major cysteine residue, the structural integrity of which is linked with an elevated rate of S-1 ATPase activation by F-actin. The noninvolvement of Cys 707 (SH1) was confirmed via further expriments. Thus, S-1 stoichiometrically labeled at this thiol with 1,5-IAEDANS, as quantitatively assessed by the incorporation of fluorescence into the tryptic 20 kDa heavy chain fragment, reacted at the same rate and to the same extent with the mixed disulfide reagent as native S-1 (data not shown). Conversely, the fluorescent dye was extensively incorporated into the same fragment of the preformed [(cysteaminyl-EDTA)Cys]S-1; also, the latter derivative underwent the dibromobimane-mediated intramolecular cross-linking between Cys 707 and Cys 522 (*27*) as efficiently as native S-1 (data not shown). (3) The presence of the EDTA function in the chemical structure of the mixed disulfide was essential for directing this reagent to the cysteine associated with F-actin activation of S-1. We have also, indeed, isolated the mixed disulfide precursor, NTB-cysteamine, and compared the kinetics of its reaction with S-1 as well as the resulting effects on the S-1 ATPases. Under identical experimental conditions, it reacted at a faster rate, and most importantly, it readily induced the inhibition of the K^+−ATPase with a parallel activation of the Ca^{2+}−ATPase (data not shown). Such alterations of both enzymatic activities represent the well-known manifestation of the chemical modification of the SH1 group in S-1 (*34*), an event that could not be observed with the EDTA-containing disulfide.

Identification of Cysteine 540 as the Major Site for Cysteaminyl-EDTA Attachment in S-1. To localize the pair of S-1 cysteines reacting with NTB-cysteaminyl-EDTA, the protein derivative produced upon exposure of S-1 (A1 and A2) for 3 h to a 2.5-fold molar excess of reagent, and containing about 1.50 mol of bound cysteaminyl-EDTA/mol of S-1, was first treated with NEM, DTE, and 5-IAF as described in Materials and Methods. This treatment ensures the blocking of the free and masked thiols of S-1 followed by the specific fluorescent labeling of the cysteine(s) reversibly engaged in a disulfide bond (*29*). Gel electrophoresis of the resulting acetamidofluorescein−S-1 revealed that the fluorescence was strongly associated with the 95 kDa heavy chain band and only slightly with both alkali light chains; no significant fluorescence pattern was noticed when the disulfide reduction with DTE was omitted or when the entire treatment was conducted with native S-1 (data not shown). The fluorescent S-1 preparation was then subjected to reverse-phase HPLC which, as described previously (*31*), led to two well-resolved protein peaks corresponding to the light chains and the heavy chain, respectively (Figure 6A). Their measured fluorescence profiles distinctly show that the fluorescence content of the heavy chain fraction was much higher than that exhibited by the light chain fraction, in agreement with the fluorescence distribution pattern initially observed on the electrophoretic gels. The fluorescent heavy chain material was pooled and extensively digested with chymotrypsin. The generated peptides were then fractionated by reverse-phase HPLC. The complete chromatogram of the digest monitored at 220 nm together with the measured

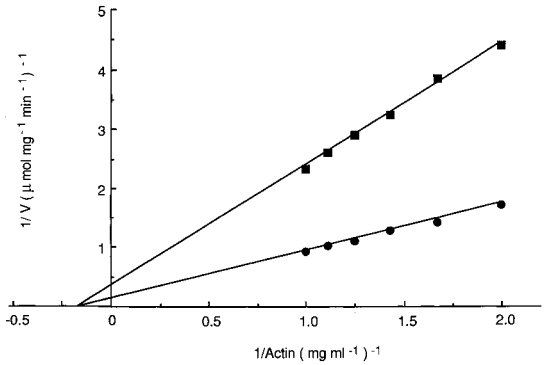

FIGURE 5: Double-reciprocal plots of the amount of activated Mg^{2+}−ATPase of [(cysteaminyl-EDTA)Cys]S-1 as a function of actin concentration. Acto-S-1 ATPase assays were performed as specified in Materials and Methods for native S-1 control (●) and for S-1 containing 1.15 mol of bound cysteaminyl-EDTA per mole of protein (■). Linear regression analysis was used to fit the data.

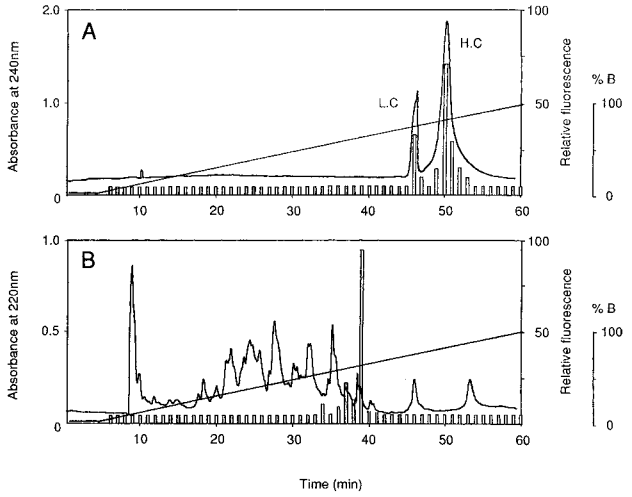

FIGURE 6: (A) Isolation by reverse-phase HPLC of the acetamidofluorescein-labeled S-1 heavy chain and alkali light chains. S-1 conjugated with 1.50 mol of cysteaminyl-EDTA/mol of protein was prepared (50 μM) and then alkylated with NEM, reduced with DTE, and labeled with 5-IAF following the procedure described in Materials and Methods. The isolated fluorescent protein (1 mL) was loaded on an aquapore C-8 Brownlee column (4 mm × 220 mm) eluted for 60 min with a gradient (0 to 100%) of solvent B consisting of 75% acetonitrile in 0.1% trifluoroacetic acid (solvent A). The fluorescence intensity (bars) of the effluent adjusted to pH 8.0 was recorded at 525 nm with excitation at 495 nm, and the fluorescent fractions of the S-1 heavy chain (H.C) and light chains (L.C) eluting between 45 and 53 min were collected for further analyses. (B) Separation of the fluorescent chymotryptic peptides from the acetamidofluorescein-labeled S-1 heavy chain. The total chymotryptic digest of the isolated fluorescent heavy chain fraction was prepared as described in Materials and Methods, and then subjected to reverse-phase HPLC using the same experimental conditions used for panel A. The two fluorescent peaks (fractions 37 and 39) were subjected to further purification as described in detail in Materials and Methods. The single fluorescent pure peptide isolated from either fraction was submitted to amino acid sequencing.

fluorescence profile is depicted in Figure 6B. A single major fluorescent peptide was eluted at fraction 39 just following the elution at fraction 37 of another minor fluorescent peptide. These two peptide fractions contained almost all the original fluorescence bound to the heavy chain. Each fraction was further purified by a reverse-phase HPLC run carried out under different elution conditions and which gave rise to a single fluorescent peptide from either fraction. Each pure peptide was submitted to microsequencing, and after 17 cycles of Edman degradation reactions, the following single sequence was obtained from either peptide, S-I-L-E-E-E-X-M-F-P-K-A-T-D-T-S-F. This sequence is consistent with that for S-1 heavy chain residues 534−550 (*35*). There was only one gap, denoted X, in the sequence, corresponding to Cys 540 of the heavy chain sequence, strongly suggesting that this residue was derivatized with acetamidofluorescein. To confirm the covalent binding of the fluorophore to this amino acid, a sample of the major fluorescent peptide was also analyzed by ionization mass spectrometry which gave a molecular mass value of 2330.0 Da, consistent with the calculated mass of 2335.53 Da for a 17-residue peptide substituted at Cys 540 with one acetamidofluorescein group. Thus, this peptide is derived from chymotryptic cleavages at Phe 533−Ser 534 and Phe 550−trimethyl Lys 551. The corresponding sequence of the S-1 heavy chain includes Cys 540, the thiol group of which must act as the unique fast reacting thiol serving for the extensive attachment of the cysteaminyl-EDTA moiety to S-1. Because this cysteine is located in the strong actin-binding motif (*16*), its modification likely causes the observed concomitant decrease of the rate of the acto-S-1 ATPase.

The fluorescent light chain fraction was also subjected to a total hydrolysis with trypsin. The reverse-phase HPLC separation of the tryptic peptides resulted in the isolation of a single fluorescent peptide which was sequenced by Edman degradation for the first 15 amino acids (data not shown). It yielded the sequence M-K-E-E-E-V-E-A-L-M-A-G-Q-E-D which identifies the penultimate C-terminal 27-residue tryptic fragment of the light chains ending with the sequence AFVK and including the single cysteine residue 177 (A1) or 136 (A2) (*36*). In native S-1, its thiol group should represent the slowly reacting sulfhydrile involved in the observed partial and noninhibitory disulfide exchange with NTB-cysteaminyl-EDTA.

Actin Site-Specific Oxidative Cleavage of the S-1 Heavy Chain. When [(cysteaminyl-EDTA)Cys]S-1 was supplemented with Fe^{3+} ions, added in an equivalent amount to the attached EDTA, and then incubated with ascorbic acid at pH 7.5 and room temperature, for up to 60 min, it exhibited, upon gel electrophoresis, the typical pattern depicted in Figure 7A. Six novel peptide bands with apparent molecular masses of 68, 62, 54, 40, 32, and 26 kDa, respectively, were accumulated within 30 min of incubation. An identical profile was obtained when the metal was chelated to NTB-cysteaminyl-EDTA before the disulfide exhange reaction between the latter reagent and S-1. The novel protein band pattern was abolished when the ascorbate or the iron was omitted or when Fe^{3+} was replaced with Mg^{2+} or Ni^{2+}; also, the addition of free Fe^{3+} and EDTA to a mixture of native S-1 and ascorbate did not change the S-1 electrophoretic profile (data not shown). The same fragment bands were formed when the S-1 derivative contained either 1 or 2 cysteaminyl-EDTA groups/mol of protein. Collectively, these findings strongly suggest that the six observed peptide species were generated by an oxidative fragmentation of the 95 kDa heavy chain mediated by the cysteaminyl-EDTA−Fe complex disulfide-linked to Cys 540 in the strong actin binding site. Their production fulfils most of the known criteria established for a site-specific chemical proteolysis (*17*−*22*). First, peptide bond cleavage was limited

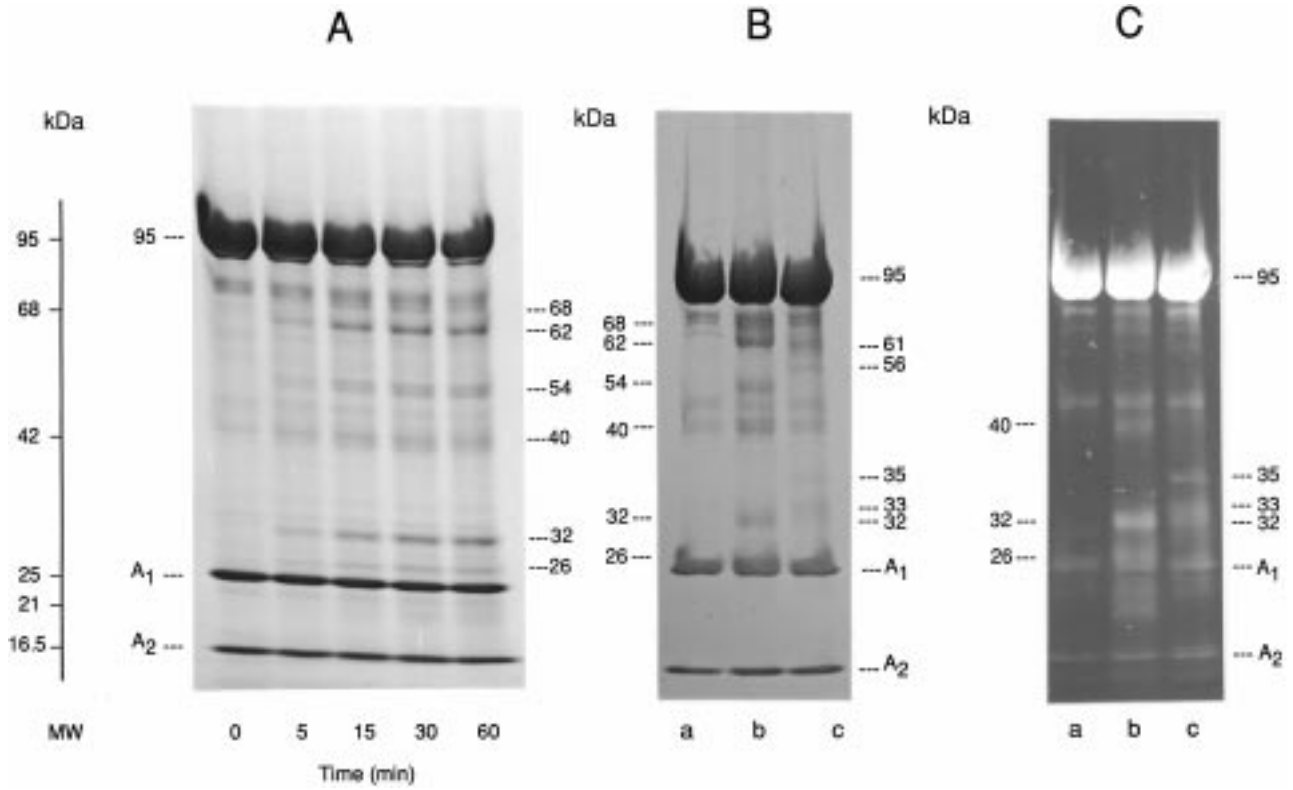

FIGURE 7: Electrophoretic analysis of the chemical cleavage fragments of [(cysteaminyl-EDTA-Fe)Cys]S-1. (A) Time course of the fragmentation reaction upon incubation of the S-1 derivative (50 μM), including 1.0 mol of cysteaminyl-EDTA−Fe/mol of protein in 20 mM MOPS and 15 mM ascorbate (pH 7.5) at 20 °C. Protein samples were subjected to $NaDodSO_4$ gel electrophoresis on a 5 to 18% gradient acrylamide gel followed by Coomassie blue staining. The protein band pattern before (lane 0) and after exposure to ascorbate for the indicated periods is shown. (B) Coomassie blue-stained electrophoretic profiles of the cleavage products formed after incubation for 30 min with ascorbate in the absence (lane b) and presence (lane c) of 0.5% $NaDodSO_4$; as a control, the derivative was incubated without ascorbate and denaturing agent (lane a). (C) The corresponding fluorescent gels (lanes a−c) viewed under UV light, using [(cysteaminyl-EDTA−Fe)Cys]S-1 labeled with 5-IAF at Cys 707 as the starting material for fragmentation. The fluorophore was incorporated into the 40, 32, and 26 kDa cleavage bands derived from the intact S-1 derivative and into the 35 and 33 kDa bands derived from the unfolded protein. The MW column depicts locations of protein molecular mass markers.

to a small amount of S-1 not exceeding 6−8%, and in practice, long overloaded gels have to be used to conveniently monitor the process. This quantitative restriction rules out extensive nonspecific protein degradation. Most importantly, it makes very likely the occurrence of a single cutting event at each protein segment involved in the fragmentation reaction. Second, there was no noticeable precursor−product relationship between the six fragments, implying that they were simultaneoulsly produced and no peptide was derived by a cleavage caused by a preceding splitting reaction. Finally, the generation of all fragments was dependent on the S-1 conformation since, as shown in lane c of Figure 7B, the fragmentation conducted in the presence of 0.5% $NaDodSO_4$ led to their suppression together with the appearance of a distinct protein band pattern consisting of peptides with apparent masses of 61, 56, 35, and 33 kDa, respectively. These components are derived only from sequence-dependent cleavage around Cys 540. No peptides that originated from the scission of the light chains were observed in the absence or in the presence of the denaturing agent.

To locate the position of the six cleavage fragments on the primary structure of the 95 kDa S-1 heavy chain, native S-1 fluorescently labeled at Cys 707 with 5-IAF was first derivatized with NTB-cysteaminyl-EDTA−Fe and then subjected to fragmentation. After gel electrophoresis, the comparison of lanes b in panels B and C of Figure 7 indicated that the fluorescence was incorporated into the 40, 32, and 26 kDa bands which must represent the C-terminal fragments of the heavy chain, whereas the 68, 62, and 54 kDa species were not at all fluorescent and must be regarded as the complementary N-terminal fragments of the heavy chain. The sum of the molecular masses for each of these three pairs of fragments (68 kDa−26 kDa, 62 kDa−32 kDa, and 54 kDa−40 kDa) accounted well for the entire mass of the intact S-1 heavy chain and was consistent with the fluorescence distribution as well as with the observed relative band intensities. Also, the two associated 54 and 40 kDa entities migrated as doublet bands, a microheterogeneity which, as previously observed during the oxidative cleavage of other proteins (*37*), reflects the splitting of the heavy chain at two or three closely adjacent peptide bonds within the same secondary structure segment surrounding the Fe atom. Thus, each peptide pair actually originates from a single cleavage event taking place at one of three vulnerable secondary structure elements spatially proximal to Cys 540.

Oxidative Cleavage of the Switch II Helix Modulated by Nucleotides and/or F-Actin. Because the cysteaminyl-EDTA substitution of Cys 540 did not perturb ATP binding and hydrolysis by S-1, we quantitatively analyzed the fragmentation patterns obtained for the S-1 derivative complexed to the nucleotides, MgATP, MgADP, or the phosphate ana-

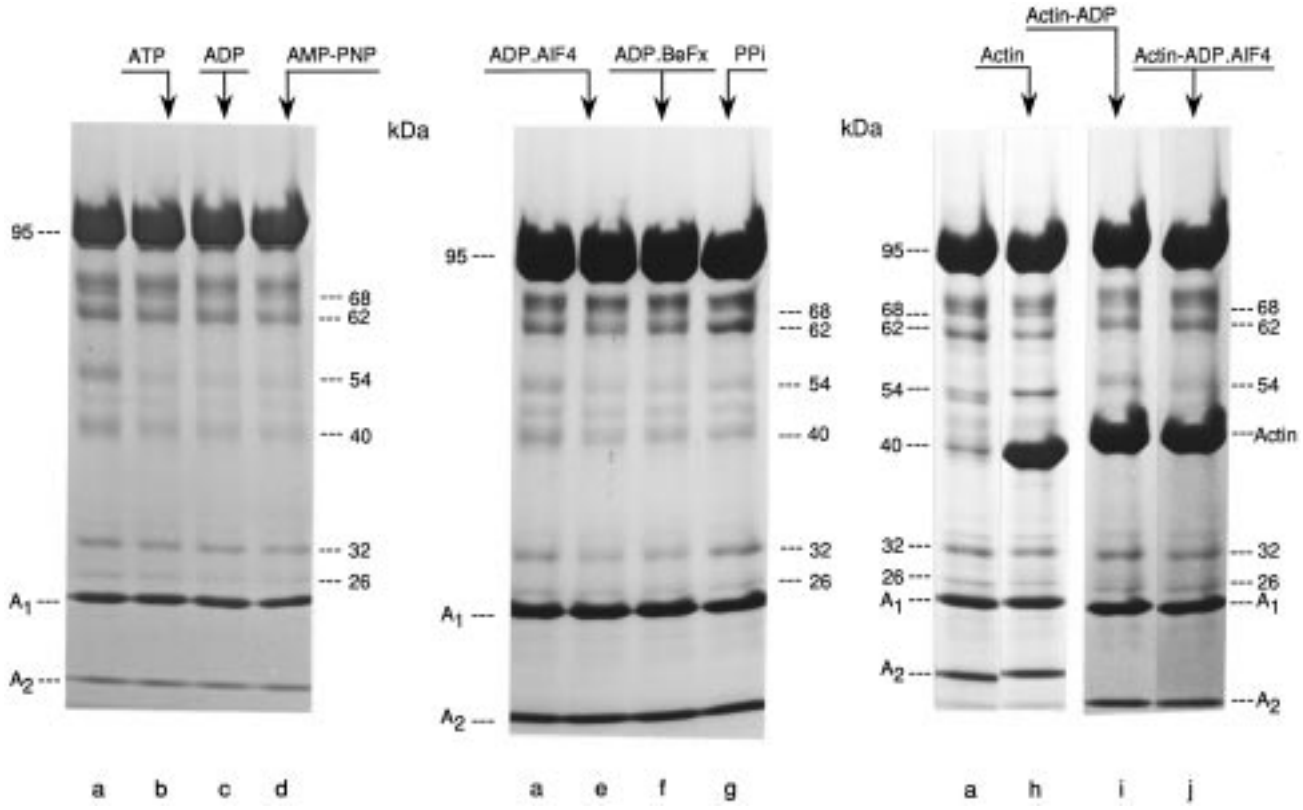

FIGURE 8: Influence of nucleotides or nucleotide analogues and/or F-actin on the fragmentation of [(cyteaminyl-EDTA−Fe)Cys]S-1. A 30 min cleavage of the S-1 derivative (40 μM) in 20 mM MOPS and 2 mM $MgCl_2$ (pH 8.0) was initiated at 20 °C by the addition of ascorbate at pH 7.2 to final concentration of 15 mM. It was conducted without any addition (lanes a) and in the presence of 2 mM ATP (lane b), 2 mM ADP (lane c), 2 mM AMP-PNP (lane d), 1 mM ADP·AlF_4 (lane e), 1 mM ADP·BeF_x (lane f), 1 mM PP_i (lane g), F-actin added at a molar ratio to S-1 of 1.0 (lane h), F-actin and 1 mM ADP (lane i), or F-actin and 1 mM ADP·AlF_4 (lane j). The ligands were introduced in the reaction medium just before the inclusion of ascorbate. All the scission reactions were analyzed via 5 to 18% gradient acrylamide gel electrophoresis.

logues $MgPP_i$, MgAMP-PNP, MgADP·BeF_x, or MgADP·AlF_4. The cleavage patterns of the modified protein complexed to F-actin in the absence and presence of MgADP or MgADP·AlF_4 were also evaluated. The overall data are presented in Figures 8 and 9. The presence of Mg^{2+} did not interfere with the fragmentation reaction because of the known very slow exchange rate between the free metal and the EDTA-bound Fe. Also, in control experiments, the addition of Mg^{2+} alone or associated with AMP, a nucleotide which does not bind to S-1, did not change the cleavage profile (data not shown). However, the inclusion of any other nucleotide or nucleotide analogue complexed to Mg^{2+} did induce a typical change in the protein band pattern. A visual inspection of the gels shown in lanes a−g Figure 8 indicated that all nucleotides or analogues afforded mainly a decrease in the band intensities associated with the 54 and 40 kDa peptides, whereas the band intensities for the two other peptide pairs were not significantly altered. The concomitant reduction of the yields for the 54 and 40 kDa species further reinforces our structural assignment for their positioning on the heavy chain sequence. On the other hand, rigor binding of F-actin to the S-1 derivative also specifically affected the magnitude of production of this particular peptide pair as reflected by an increase in the intensity of the 54 kDa band together with a virtual suppression of its doublet character (Figure 8, lane h). The parallel change in the 40 kDa band could not be appreciated as this species comigrated with actin. Furthermore, the yield increase for the 54 kDa peptide was neutralized when MgADP was combined with the rigor complex (Figure 8, lane i), and the peptide production was even strongly inhibited upon addition of MgADP·AlF_4, the putative transition state analogue, to the acto-S-1 complex (Figure 8, lane j). Multiple densitometric measurements of several series of gels led to the reproducible quantitative diagrams depicted in panels A and B of Figure 9. They clearly indicate that the extent of the change in the yield of the 54 and 40 kDa product was essentially ligand-specific depending on the composition of the binary or ternary complex being tested. Thus, for the former peptide, S-1−ADP and S-1−AMP-PNP exhibited the lowest yield (35 and 41%, respectively), followed by S-1−ADP·AlF_4 (47%), S-1−ATP (51%), S-1−ADP·BeF_x (64%), and S-1−PP_i which gave the weakest effect (95%); the same quantitative trend was observed for the complementary 40 kDa peptide (Figure 9A). In the rigor acto-S-1, the 54 kDa fragment level was enhanced to 125%, but it moderately decreased upon addition of ADP (85%) and more significantly upon association with ADP·AlF_4 (25%) to form the putative transition state analogue complex of the acto-S-1 ATPase reaction mimicking acto-S-1−ADP·P_i (Figure 9B). In contrast, the measured variation of the intensity values for the accompanying 62 kDa−32 kDa bands taken as controls was within experimental error (±15%). These data are significant as they were observed with different modified S-1 peparations and following several independent densitometric determinations. They could be best interpreted by assuming

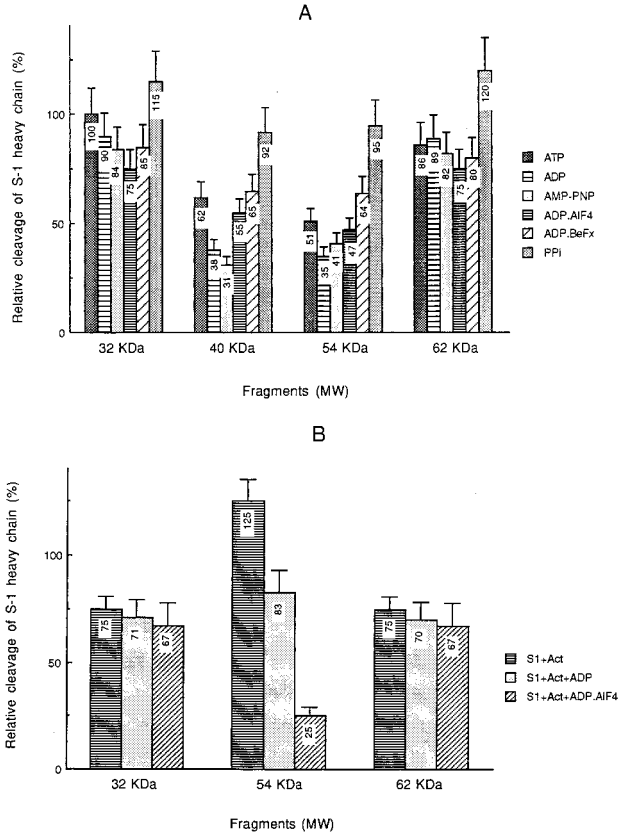

FIGURE 9: Measurements of the changes in the yield of the 54 kDa−40 kDa pair of fragments during the cleavage of [(cysteaminyl-EDTA−Fe)Cys]S-1 in the presence of various ligands. (A) Densitometric measurements of the band intensities in several sets of gels, obtained under the experimental conditions described in the legend of Figure 8, were performed to reproducibly quantify the average percents of nucleotide- or nucleotide analogue-induced decrease in the magnitude of production of the 54 kDa−40 kDa pair of fragments relative to the S-1 derivative cleaved without ligands. The average intensities of the 62 kDa−32 kDa pair of bands were also estimated as controls. The bars include the average values of at least three separate determinations, and the error bars represent the standard deviation. (B) The average percentages of yield change induced by F-actin alone or combined with MgADP or MgADP·AlF_4 for the production of the 54 kDa fragment and the accompagnying 62 kDa−32 kDa bands are also presented. The experimental conditions were as described in the legend of Figure 8. The values that are shown are the average ± standard deviation determined from three independent densitometric measurements.

that the binding of each ligand to the S-1 derivative causes a distinct conformational change in the secondary structure element whose cleavage releases the 54 kDa−40 kDa pair of peptides. Such a structural transition definitely alters the orientation and/or solvent accessibility of the susceptible polypeptide segment, thereby modulating its cleavage efficiency.

In an attempt to directly characterize the ligand-responsive cleavage region, the 54 and 40 kDa fragments were isolated by gel electrophoresis combined with reverse-phase HPLC and subjected to end group analyses. However, N-terminal sequencing of the latter C-terminal peptide and digestion with carboxypeptidase γ of the former N-terminal material were not successful. This finding was not unexpected because cleavage fragments with both free terminal ends (*17*, *22*) and blocked terminal ends (*38*, *39*) have been reported previously, depending on the reaction mechanism which would be hydrolytic in the former case and oxidative in the latter case (*38*, *39*). One of the proposed oxidative pathways yields an N-terminal fragment with a C-terminal amide and a C-terminal fragment with a blocked N-terminus, thus explaining our own data. Nevertheless, the examination of the crystal structure of the S-1 catalytic domain, as shown in Figure 10, unequivocally identifies the N-terminal portion of the switch II helix around Leu 475 as the only heavy chain segment located within the dynamic span (5−15 Å) of the EDTA−Fe arm tethered to Cys 540, which could be cleaved to generate a pair of 54 and 40 kDa peptides. The Cα of Leu 475 lies 14.19 Å from Cys 540, and the mass assigned to the former fragment matches that calculated for the sequence of amino acids 1−475 (53 560 Da) (*35*). The distances from Cys 540 to the backbones of residues Glu 476 and Ser 474, flanking Leu 475, are 16.72 and 16.94 Å, respectively. The dynamic properties in solution of the polypeptide chain could put both distances within the maximum physical reach of the EDTA−Fe with potential cleavages at the corresponding peptide bonds. These properties could also favor the cleavage of the helix at a range of residues as suggested by the doublet nature of the 54 and 40 kDa fragments. In contrast, the distances from Cys 540 to the backbones of residues 468−473, making part of the switch II loop, are much larger (>22 Å), ruling out any fragmentation at this loop. Because the switch II helix binds neither to nucleotides nor to actin (*3*, *16*), the observed specific modulation by these ligands of its cleavage amplitude at the proposed sites is not a direct steric effect but rather the manifestation of the crucial allosteric role imparted to this motif in the communication between the ATPase site and the actin binding site during energy transduction (*40*).

DISCUSSION

An initial important step in this work was the rapid synthesis of NTB-cysteaminyl-EDTA and its successful targeting to Cys 540 in the strong actin binding motif of skeletal myosin-S-1. The previously reported cysteaminyl-EDTA-containing mixed disulfides were prepared exclusively in organic solvents using relatively long and expensive procedures (*17*, *20*, *21*). The simple and very rapid synthesis in aqueous solution we have described for NTB-cysteaminyl-EDTA makes this reagent readily available for processing at will the specific derivatization of protein thiols with the EDTA−Fe chelate. To serve as a site-directed chemical catalyst of peptide bonds hydrolysis, the latter complex needs to be covalently attached at a well-defined amino acid on the polypeptide chain. To satisfy this requirement, use is often made of protein recombinants with a single engineered cysteine at the desired position. However, this study showed that the disulfide−thiol interchange reaction between our reagent and native rabbit S-1 exhibited the remarkable property of causing the rapid substitution of Cys 540 without modification of any other sulfhydryl on the heavy chain, including the so-called reactive SH1−SH2 groups. Recent investigations have emphasized the important role of electrostatic interactions between charged groups of the protein and disulfide reagents in determining the rate of the exchange reaction, thereby favoring or inhibiting the formation of a disulfide bond at a particular protein thiol (*41*). We have found that only the EDTA-containing mixed disulfide did specifically react with Cys 540. The EDTA moiety comprises

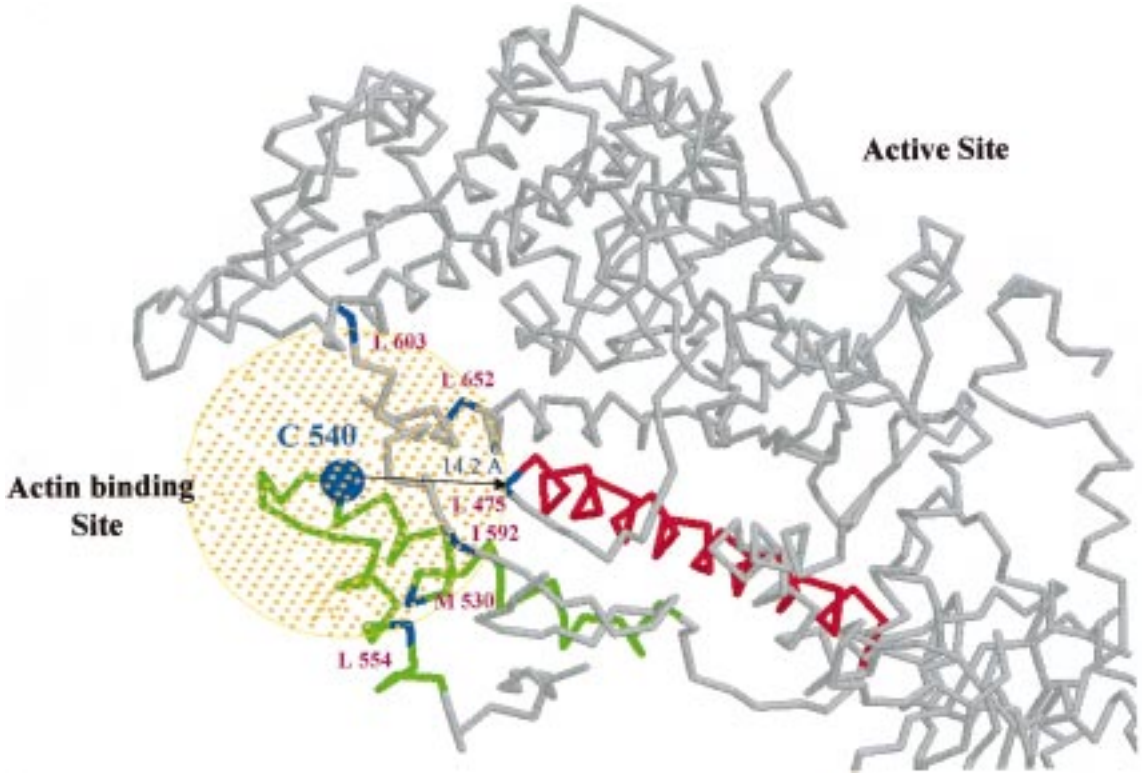

FIGURE 10: Cα trace of the heavy chain in the catalytic domain of chicken skeletal myosin S-1 with the cysteaminyl-EDTA−Fe complex (black arrow) disulfide-linked to Cys 540 (blue sphere). The yellow circle and the yellow cloud it contains represent the maximum length (≅15 Å) of the latter flexible complex and the allowed iron positions in space, respectively. The strong actin-binding helix−loop−helix motif of residues 516−558 (green) and the switch II helix of residues 475−507 (red) are shown. Potential cleavage sites (blue lines), within the reach of the EDTA−Fe chelate, include Leu 475 at the N-terminus of the switch II helix, 14.2 Å from Cys 540, that would be the ligand-sensitive site for the generation of the 54 kDa−40 kDa peptides. The scission at the other sites within different secondary structure segments may account for the production of the 68 kDa−22 kDa and 62 kDa−32 kDa pairs of fragments. The Cα coordinates of S-1 were kindly supplied by I. Rayment.

a cluster of three negatively charged carboxyls which could drive the reagent to Cys 540 by interacting, in a first stage of the reaction, with conveniently oriented positive charges in the vicinity of this residue. A potential positively charged heavy chain segment is the lysine-rich 50 kDa−20 kDa junction loop of residues 627−646 which is known to bind to the negatively charged carboxyl side chains at the N-terminus of actin (*16*). In a recent new model of the skeletal rigor acto-S-1 complex (*42*), the predicted structure established for this loop was clearly placed very close to the C-terminus of the helix from Gly 516 to Phe 542, making part of the strong actin binding motif of S-1. Thus, by first associating to the loop and then to the nearby Cys 540, the NTB-cysteaminyl-EDTA would somewhat mimic actin, which also sequentially binds to the same sites during the ATPase cycle, and in doing so, the reagent would behave as a potent actin site-directed thiol modifier of the skeletal myosin motor. In the course of this study, we have also similarly synthesized another mixed disulfide analogue which included, besides the metal-binding tricarboxylic motif, the fluorescent AEDANS group. Preliminary experiments indicated that, under the standard conditions used with NTB-cysteaminyl-EDTA, this compound modifies even more specifically S-1 as its fluorescence was incorporated exclusively into the tryptic 50 kDa heavy chain fragment containing Cys 540 and unsignificantly into the light chains. Mixed disulfides of this class make possible direct fluorescence or luminescence spectroscopy studies of the strong actin binding site of skeletal S-1 as well as of any other S-1 mutant bearing a single engineered cysteine at this critical location (*43*). In this regard, the investigation presented here extends our previous work describing the selective fluorescent labeling of Lys 553 residing at the end of the strong actin binding motif (*31*).

For the cysteaminyl-EDTA to specifically mediate the conformation-dependent cleavage of S-1 heavy chain segments spatially close to Cys 540, its introduction at this residue should not alter the major biological properties of the protein. Our data indicated that it did not perturb the S-1 ATPase site but only moderatly reduced the maximum rate of the acto-S-1 ATPase reaction without affecting the affinity of the S-1−ATP complex for F-actin. It is unlikely that the observed effect on the actin activation of S-1 was caused by the ability of Cys 540 to act as an essential structural determinant of the strong actin binding site because this residue is not strictly conserved in the myosin sequences being replaced by different amino acids (*44*). However, Cys 540 is located just adjacent to the highly conserved cluster of acidic residues 537−539 thought to be crucial for actin recognition (*45*). Interestingly, earlier, a point mutation at the position of Glu 538 in the *Dictyostelium* myosin II (Glu 531 → Gln) also caused mainly a decrease in the actin activation rate without affecting ATP binding and hydrolysis, as we observed with S-1 modified at Cys 540 (*46*). This effect was shown to be linked with a 10-fold reduction in the rigor binding affinity of the mutant for F-actin. Although we did observe that at least 90% of our modified S-1 could be sedimented with F-actin in the absence of ATP, we did

not measure the strength of this interaction. Thus, it is quite possible that the small and flexible cysteaminyl-EDTA tethered to Cys 540 has partially interfered with the full binding of actin to the adjacent acidic motif of residues 537−539 slowing the rate of the transition between the weakly and strongly bound states of the acto-S-1 complex, thereby causing the observed reduction of the V_{max} of the acto-S-1 ATPase.

A further significant step in the work was the activation of the EDTA−Fe chelate bound to Cys 540 by ascorbate with a concomitant site-specific cleavage of the S-1 heavy chain at three secondary structure elements located in the tertiary structure within a radius of about 15 Å from this residue. The three pairs of fragments that are produced reflect the native state of S-1 as they are all suppressed when the fragmentation was performed on the denatured protein. They did not result from oxidative damage of amino acid side chains along the heavy chain, as previous studies have shown that the level of potential EDTA−Fe-promoted side chain oxidation was low and most cleavage events are thought to occur in unoxidized protein populations (*17*). Thus, the level of generation of each peptide pair mainly monitors the degree of solvent exposure of the cleavable peptide bonds and/or the degree of their accessibility to the diffusible reactive oxygen species. Conformational changes in the secondary structure segments harboring the cleavage sites are expected to alter the hydrolytic susceptibility of these sites and to change the amounts of released peptides and/or the fragmentation pattern itself (*17*). Our results revealed that the yield of the peptide pair comprising the 54 and 40 kDa heavy chain fragments was particularly sensitive to S-1 binding to nucleotides, nucleotide analogues, and/or F-actin which either decreased or increased the extent of formation of these two peptides in a ligand-specific manner. We assigned the corresponding cleavage region to the polypeptide backbone at the N-terminus of the switch II helix around Leu 475. The proposed ligand-induced movements of this segment are consistent with reported deleterious effects of its mutation on the myosin function (*47*). Thus, mutagenesis of *Dictyostelium* myosin at Ser 474 (Ser 465 → Val) resulted in the partial uncoupling of ATPase and in vitro motility. Also, the segment is in the center of the region between Leu 453 and Phe 482 which makes several important contacts during ATP hydrolysis (*45*). On the other hand, the likely propagation of the movements induced by all nucleotides and analogues along the switch II helix until its C-terminus at residue 507 would rationalize the change in the environment of the nearby Trp 510 observed in solution upon S-1 binding not only to ATP but also to ADP and AM-PPNP (*48*). The increased cleavage yield and change in the 54 kDa−40 kDa band pattern with the acto-S-1 complex are the first direct manifestations of the predicted influence of F-actin on the switch II helix structure. It is possible that actin stabilizes a particular conformation of the helix having a greater propensity for cleavage at a single site. The decrease in the cleavage yield distinguished not only the two types of helix structural states corresponding to S-1−ADP·AlF_4 and S-1−ADP but also the two different helix conformations associated with F-actin−S-1−ADP·AlF_4, the putative transition state analogue complex of the acto-S-1 ATPase, and F-actin−S-1−ADP. Although each suggested helix conformation might not necessarily be accompanied by a motion of the lever arm domain, the detection of the two latter important states of the helix is consistent with recent luminescence energy transfer data which indicate that the transition between these two complexes, thought to represent the pre-power stroke state and the post-power stroke state, respectively, generates the most substantial movement of the lever arm domain (*49*). In this regard, it is noteworthy that the largest difference in the cleavage yield was also observed between these two complexes (25 vs 80%). Furthermore, the distinct helix conformation detected for acto-S-1−ADP as compared to acto-S-1 is in line with recent X-ray studies suggesting a small axial movement of the lever arm domain upon binding of ADP to the rigor actomyosin complex of rabbit skeletal muscle (*50*). Thus, in several cases there is a correlation between the particular conformation of the switch II helix detected by the proteolytic probe and a defined structural state of the lever arm domain reported previously. This observation strengthens the proposal for the essential role of this motif in the communication of the nucleotide-promoted conformational changes in the catalytic domain to the latter amplifier domain of the S-1 molecule (*2*).

Because proteolysis is, in general, a highly sensitive probe of the protein conformation, the actin site-specific chemical cleavage, which we have employed, appears to be a valuable tool for assessing in solution the structural transitions of modest amplitude taking place in the switch II helix during the functioning of the acto-S-1−ATP complex. As some of these transient conformations could escape trapping in the S-1 crystal, our approach usefully complements the crystallographic analyses of the protein.

REFERENCES

1. Rayment, I., Rypniewski, W. R., Schmidt-Bäse, K., Smith, R., Tomchick, D. R., Benning, M. M., Winkelmann, D. A., Wesenberg, G., and Holden, H. M. (1993) *Science 261*, 50−58.
2. Fisher, A. J., Smith, C. A., Thoden, J., Smith, R., Sutoh, K., Holden, H. M., and Rayment, I. (1995) *Biophys. J. 68*, 19s−28s.
3. Fisher, A., Smith, C., Thoden, J., Smith, R., Sutoh, K., Holden, H., and Rayment, I. (1995) *Biochemistry 34*, 8960−8972.
4. Rayment, I. (1996) *J. Biol. Chem. 271*, 15850−15853.
5. Gulick, A. M., Bauer, C. B., Thoden, J. B., and Rayment, I. (1997) *Biochemistry 36*, 11619−11628.
6. Smith, C. A., and Rayment, I. (1996) *Biochemistry 35*, 5404−5417.
7. Smith, C. A., and Rayment, I. (1995) *Biochemistry 34*, 8973−8981.
8. Whittaker, M., Wilson-Kubalek, E. M., Smith, E. J., Faust, L., Milligan, R. A., and Sweeney, H. L. (1995) *Nature 378*, 748−751.
9. Reisler, E., Burke, M., Mimmelfarb, S., and Harrington, W. F. (1974) *Biochemistry 13*, 3837−3840.
10. Burke, M., and Reisler, E. (1977) *Biochemistry 16*, 5559−5563.
11. Wells, J. A., Knoeber, C., Sheldon, M. C., Werber, M. M., and Yount, R. G. (1980) *J. Biol. Chem. 255*, 11135−11140.
12. Wells, J. A., and Yount, R. G. (1980) *Biochemistry 19*, 1711−1717.
13. Miller, L., Coppedge, J., and Reisler, E. (1982) *Biochem. Biophys. Res. Commun. 106*, 117−122.
14. Polosukhina, K., and Highsmith, S. (1997) *Biochemistry 36*, 11952−11958.
15. Nitao, L. K., and Reisler, E. (1998) *Biochemistry 37*, 16704−16710.

16. Rayment, I., Holden, H. M., Whittaker, M., Yohn, C. B., Lorenz, M., Holmes, K. C., and Milligan, R. A. (1993) *Science 261*, 58−65.
17. Ermacora, M. R., Delfino, J. M., Cuenod, B., Schepartz, A., and Fox, R. O. (1992) *Proc. Natl. Acad. Sci. U.S.A. 89*, 6383−6387.
18. Ermacora, M. R., Ledman, D. W., Hellinga, H. W., Hsu, G. W., and Fox, R. O. (1994) *Biochemistry 33*, 13625−13641.
19. Ermacora, M. R., Ledma, D. W., and Fox, R. O. (1996) *Nat. Struct. Biol. 3*, 59−66.
20. Ebright, Y. W., Chen, Y., Pendergrast, P. S., and Ebright, R. H. (1992) *Biochemistry 31*, 10664−10670.
21. Flaus, A., Luger, K., Tan, S., and Richmond, T. J. (1995) *Proc. Natl. Acad. Sci. U.S.A. 93*, 1370−1375.
22. Rana, T. M., and Meares, C. F. (1991) *Proc. Natl. Acad. Sci. U.S.A. 88*, 10578−10582.
23. Offer, G., Moss, C., and Starr, R. (1973) *J. Mol. Biol. 74*, 653−679.
24. Chaussepied, P., Mornet, D., Audemard, E., Derancourt, J., and Kassab, R. (1986) *Biochemistry 25*, 1134−1140.
25. Eisenberg, E., and Kielley, W. W. (1974) *J. Biol. Chem. 249*, 4742−4748.
26. Duke, J., Takashi, R., Ue, K., and Morales, M. F. (1976) *Proc. Natl. Acad. Sci. U.S.A. 73*, 302−306.
27. Mornet, D., Ue, K., and Morales, M. F. (1985) *Proc. Natl. Acad. Sci. U.S.A. 82*, 1658−1662.
28. Riddles, P. W., Blakeley, R. L., and Zerner, B. (1983) *Methods Enzymol. 91*, 49−61.
29. Gitler, C., Zarmi, B., and Kalef, E. (1997) *Anal. Biochem. 252*, 48−55.
30. Laffite, D., Capony, J. P., Grassy, G., Haiech, J., and Calas, B. (1995) *Biochemistry 34*, 13825−13832.
31. Bertrand, R., Derancourt, J., and Kassab, R. (1995) *Biochemistry 34*, 9500−9507.
32. Bertrand, R., Derancourt, J., and Kassab, R. (1997) *Biochemistry 36*, 9703−9714.
33. Faulstich, H., Tews, P., and Heintz, D. (1993) *Anal. Biochem. 208*, 357−362.
34. Reisler, E. (1982) *Methods Enzymol. 85*, 84−93.
35. Tong, S.-W., and Elzinga, M. (1990) *J. Biol. Chem. 265*, 4893−4901.
36. Frank, G., and Weeds, A. G. (1974) *Eur. J. Biochem. 44*, 317−334.
37. Multhaup, G., Ruppert, T., Schlicksupp, A., Hesse, L., Bill, E., Pipkorn, R., Masters, C. L., and Beyreuther, K. (1998) *Biochemistry 37*, 7224−7230.
38. Platis, I. E., Ermacora, M. R., and Fox, R. O. (1993) *Biochemistry 32*, 12761−12767.
39. Gallagher, J., Zelenko, O., Walts, A. D., and Sigman, D. S. (1998) *Biochemistry 37*, 2096−2104.
40. Cooke, R. (1997) *Physiol. Rev. 77*, 671−697.
41. Bulaj, G., Kortemme, T., and Goldenberg, D. P. (1998) *Biochemistry 37*, 8965−8972.
42. Mendelson, R., and Morris, E. P. (1997) *Proc. Natl. Acad. Sci. U.S.A. 94*, 8533−8538.
43. Shih, W. M., and Spudich, J. A. (1998) *Biophys. J. 74*, 259a.
44. Sellers, J. R., and Goodson, H. V. (1995) *Protein Profile 2*, 1327−1330.
45. Cope, M. J., Whisstock, J., Rayment, I., and Kendrik-Jones, J. (1996) *Structure 4*, 969−987.
46. Giese, K. C., and Spudich, J. A. (1997) *Biochemistry 36*, 8465−8473.
47. Ruppel, K. M., and Spudich, J. A. (1996) *Mol. Biol. Cell 7*, 1123−1136.
48. Onishi, H., Kojima, S., Katoh, K., Fujiwara, K., Martinez, H. M., and Morales, M. F. (1998) *Proc. Natl. Acad. Sci. U.S.A. 95*, 6653−6658.
49. Xiao, M., Li, H., Snyder, G. E., Cooke, R., Yount, R. G., and Selvin, P. R. (1998) *Proc. Natl. Acad. Sci. U.S.A. 95*, 15309−15314.
50. Xu, S., Gu, J., Frisbie, S., and Yu, L. C. (1998) *Biophys. J. 74*, 363a.

BI9909896